



Comprehensive analysis of mutational profile and prognostic significance of complex glandular pattern in lung adenocarcinoma

Jinsong Bai^{1,2,3#}, Chaoqiang Deng^{1,2,3#}, Qiang Zheng^{2,3,4}, Di Li^{1,2,3}, Fangqiu Fu^{1,2,3}, Yuan Li^{2,3,4}, Yang Zhang^{1,2,3}, Haiquan Chen^{1,2,3}

¹Department of Thoracic Surgery and State Key Laboratory of Genetic Engineering, Fudan University Shanghai Cancer Center, Shanghai, China;

²Institute of Thoracic Oncology, Fudan University, Shanghai, China; ³Department of Oncology, Shanghai Medical College, Fudan University, Shanghai, China; ⁴Department of Pathology, Fudan University Shanghai Cancer Center, Shanghai, China

Contributions: (I) Conception and design: H Chen, Y Zhang, Y Li; (II) Administrative support: H Chen, Y Zhang, Y Li; (III) Provision of study materials or patients: J Bai, C Deng, Q Zheng, D Li, F Fu, Y Li; (IV) Collection and assembly of data: J Bai, C Deng, Q Zheng, D Li, F Fu, Y Li; (V) Data analysis and interpretation: J Bai, C Deng, F Fu; (VI) Manuscript writing: All authors; (VII) Final approval of manuscript: All authors.

[#]These authors contributed equally to this work.

Correspondence to: Yang Zhang; Haiquan Chen. Department of Thoracic Surgery, Fudan University Shanghai Cancer Center, 270 Dong-An Road, Shanghai 200032, China. Email: fdzhangyang1987@hotmail.com; hqchen1@yahoo.com.

Background: Complex glandular pattern (CGP) was included as high-grade pattern in the new grading system proposed by The International Association for the Study of Lung Cancer. We aimed to investigate the mutational profile and validate the prognostic significance and proper cut-off value to distinguish the aggressive behavior of CGP.

Methods: CGP was defined as nests of tumor cells with sieve-like perforation, fused glands with irregular borders or back-to-back glands without intervening stroma. Patients were categorized into four groups according to the percentage of CGP component (0%, 1–19%, 20–49%, 50–100%). Cox's proportional hazards model was applied to analyze recurrence free survival (RFS) and overall survival (OS).

Results: A total of 950 patients with resected lung adenocarcinoma was enrolled. The most frequent driver mutation in this cohort was *EGFR* and was detected in 624 (65.7%) patients. *EGFR* mutation was more frequently observed in patients with <20% CGP than in patients with ≥20% CGP (73.6% vs. 60.2%), while *KRAS* mutation and *ALK* rearrangement was significantly associated with ≥20% CGP. Patients with 20% or greater CGP exhibited significant worse RFS ($P < 0.001$) and OS ($P < 0.001$) than their counterparts. Moreover, the multivariate Cox regression analysis confirmed that CGP (≥20%) was a risk factor for a worse RFS ($P = 0.001$) and OS ($P < 0.001$) independent of staging and gene mutation. Smaller portion of CGP (<20%) were comparable in RFS and OS to those without CGP (0%). There was also no significant difference in RFS and OS between the 20–49% and ≥50% group.

Conclusions: Our study provided mutational profile of patients with different CGP, validated CGP as a negative prognostic factor and provided extra evidences for the optimal cut-off value of CGP percentage.

Keywords: International Association for the Study of Lung Cancer grading system (IASLC grading system) grading system; driver mutations; complex glandular pattern (CGP); pulmonary adenocarcinoma

Submitted Jan 17, 2022. Accepted for publication Jun 01, 2022.

doi: 10.21037/tlcr-22-127

View this article at: <https://dx.doi.org/10.21037/tlcr-22-127>

Introduction

Lung cancer ranks as one of the most frequent cancer worldwide, and is associated with extremely high morbidity and mortality (1). According to the 2015 World Health Organization (WHO) lung tumor classification, the predominant pathological subtype has been identified as a prognostic indicator for patients with resected lung adenocarcinoma (2-4). Other than the five major histologic patterns, new patterns have been recognized in lung adenocarcinoma, which include cribriform (nests of tumor cells with sieve-like perforation) and fused gland (fused glands with irregular borders, back-to-back glands without intervening stroma, or ribbon-like formations). Both of them were combined into complex glandular patterns (CGPs). CGP was reported to carry a poor prognosis comparable to that of high-grade histologic types (5-9) and therefore was included in the grading system proposed by International Association for the Study of Lung Cancer grading system (IASLC) as high-grade pattern, together with solid and micropapillary pattern (10,11). The new grading system proposed that any tumor with 20% or more of high-grade patterns be classified as poorly differentiated (10). As a “nontraditional pattern”, CGP has not been widely applied and appreciated in clinical practice. Therefore, we found it necessary to investigate the mutational profile related with CGP, identify its optimum cut-off value for survival discrimination and explore the potential role of CGP in clinical management.

We analyzed a series of 950 patients with resected lung adenocarcinoma, described its correlation with genetic variation and investigated its prognostic significance and proper cut-off value to distinguish its aggressive behavior. We present the following article in accordance with the REMARK reporting checklist (available at <https://tclr.amegroups.com/article/view/10.21037/tclr-22-127/rc>).

Methods

Patients

The study was conducted in accordance with the Declaration of Helsinki (as revised in 2013). This study was approved by the institutional review board (Fudan University Shanghai Cancer Center IRB 2008223-9, date: 2020/07/14). Informed consents were waived because it was a retrospective study. We retrospectively reviewed the medical records of patients who underwent lung cancer resection at Fudan University Shanghai Cancer

Center (FUSCC) from January 2008 to September 2016. The inclusion criteria were as follows: (I) lung invasive adenocarcinoma; (II) pathological slides and driver mutation data available; We reviewed patient medical records to gain clinicopathological factors, including patient age at diagnosis, gender, smoking history, CT appearance according to thin-section computed tomography (TSCT) scan, operation procedure, TNM staging according to the eighth edition of American Joint Committee on Cancer staging manual, lymphatic vessel invasion (LVI), visceral pleura invasion (VPI) and adjuvant therapies. Overall survival (OS) was considered to be the time between the day of surgery and the day of death or last follow-up. Deaths from other causes were considered as censored. OS were recorded based on telephone follow-up for clinic visit. Recurrence-free survival (RFS) was defined as the time from the day of surgery to the day of first recurrence or last follow-up. Patients who died from other causes were considered to be censored with no event when calculating RFS. Diagram of recruitment of eligible patients were present in [Figure S1](#). The duration of follow-up ranged from one to ten years. Mean duration of follow-up was 4.6 years.

Histological evaluation

All resected specimens were formalin fixed immediately after resection and stained with H&E. The slides were evaluated independently by two pathologists who were blinded to the clinical data. Disagreements were resolved by a senior pathologist. The evaluation criterion was according to the WHO and IASLC classification of adenocarcinoma. The criteria for the CGP were consistent with Moreira *et al.* (12). CGP were divided into cribriform pattern (invasive tumor nests of tumors cells that produce glandular lumina without solid components) and fused gland pattern (invasive back-to-back fused tumor glands with poorly formed glandular spaces lacking intervening stroma). Representative figures are presented in [Figure 1](#). Patients were categorized by the proportion of CGP into four groups, 0%, 1–19%, 20–49% and 50–100%. IASLC proposed a new grading system for invasive lung adenocarcinoma in which 20% or more of high-grade patterns (including CGP) were classified as poorly differentiated. In this study, we utilize the cut-off value of 20% to validate the newly proposed grading system. To further evaluate the prognostic significance of higher CGP component, we choose 50% for its convenience in pathological evaluation.

LVI was defined as the presence of tumor emboli in

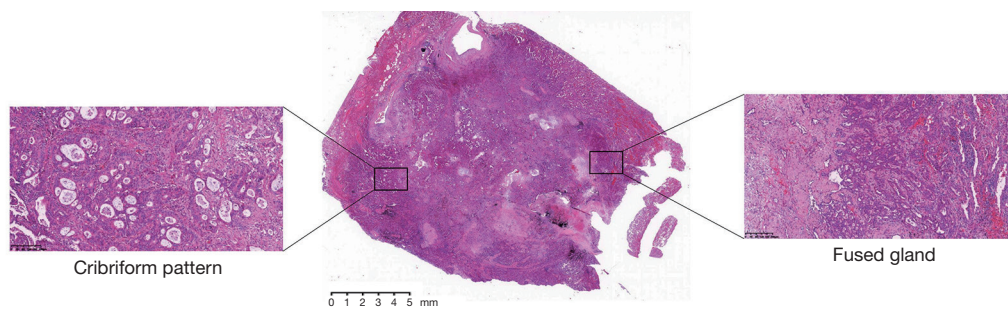


Figure 1 Histological examples in hematoxylin and eosin (HE) staining of complex glandular patterns. Left: cribriform pattern: invasive tumor nests of tumor cells that produce glandular lumina without solid components. Right: fused gland pattern: invasive back-to-back fused tumor glands with poorly formed glandular spaces lacking intervening stroma.

lymphatic or blood vessel lumens. Hematoxylin and eosin (HE) staining were performed to examine LVI status. VPI was defined as invasion of the tumor beyond the elastic layer or to the pleural surface but not to the parietal pleura. HE-stained specimens were primarily observed to evaluate visceral pleural invasions. For undetermined cases, elastic fiber stains were performed to ascertain.

Mutational analysis

Mutation analysis procedure was performed as previous studies (13,14). *ALK*, *ROS1* and *RET* translocations were detected by quantitative real-time reverse transcriptase PCR (qRT-PCR)-based fusion detection methods. Validation was made using fluorescent *in situ* hybridization (FISH). We designed reverse transcriptase polymerase chain reaction (RT-PCR) primers to cover mutation hot-spot regions of common driver genes concerning *EGFR* (exons 18 to 22), *HER2* (exons 18 to 21), *KRAS* (exons 2 to 3) and *BRAF* (exons 11 to 15). Sanger sequencing was used to analyze the PCR amplified products.

Statistical analysis

The χ^2 test was applied to compare the association between cribriform pattern and clinical features as well as several genetic variations. The RFS and OS were investigated using the Kaplan-Meier method and log-rank test was employed to compare differences between groups. The association between CGP component and postoperative recurrence was also analyzed using competing risk regression model of Fine and Gray. Univariate and multivariable analyses for the association with recurrence risk of the patients were performed using the Cox regression hazards model.

Variables with a P value less than 0.10 in univariate analysis or variables we deem relevant were used in the multivariate survival analysis. A two-tailed P value less than 0.05 was considered statistically significant for interpretation of the results. Statistical analyses were performed using IBM SPSS version 23.0 (SPSS, Chicago, IL) and R Statistical Language (version 3.6.1).

Results

Patient characteristics and association with CGP

Patients were divided into four groups according to the percentage of CGP component (0%, 1–19%, 20–49%, 50–100%). There were 109 patients with 0% CGP, 278 patients with 1–19% CGP, 407 patients with 20–49% CGP and 156 patients with 50–100% CGP (Figure 2). Important clinicopathological findings for all patients as well as comparisons among groups (0–19% and 20–100%) are summarized in Table 1. CGP was significantly associated with male gender ($P=0.004$), smoking history ($P<0.001$), absence of ground-glass opacity (GGO) component ($P<0.001$), higher TNM stage (including pT and pN stages) ($P<0.001$), visceral pleura invasion (VPI) ($P<0.001$) and lymphatic vessel invasion (LVI) ($P<0.001$).

Prognostic significance of CGP

In all patients, 20% or greater CGP was significantly associated with worse RFS (mean RFS: 36.4 vs. 52.8 months, $P<0.001$) and OS (mean OS: 47.6 vs. 57.4 months, $P<0.001$) (Figure 3). Competing risks models for postoperative recurrence were also performed in all stages and stage I patients (Figure S2). It's rather clear that CGP is associated

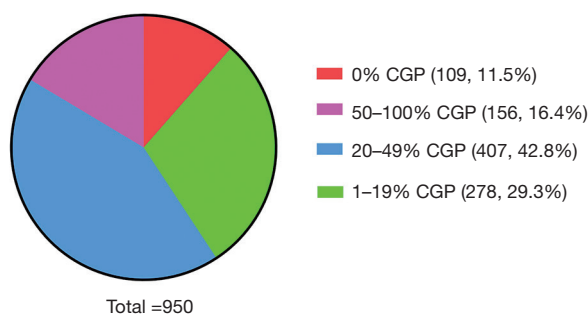


Figure 2 Distribution of different CGP component (0%, 1–19%, 20–49% and 50–100%) in the whole cohort. CGP, complex glandular pattern.

with higher-staged adenocarcinoma, therefore, we performed survival analysis of RFS and OS in a subgroup of stage I patients, the results were consistent with the whole cohort. However, in stage II and III patients, 20% CGP did not stratify RFS or OS (*Figure 3*).

To investigate the prognostic significance of CGP component level, we analyzed smaller portion of CGP (<20%) and found that they were comparable in RFS and OS to those without CGP (0%) (*Figure 4*). Prognosis of greater complex glandular component was also analyzed, and we found that there was no significant difference in RFS and OS between 20–45% CGP and ≥50% CGP. In a subgroup of stage I patients, the prognostic significance of the CGP was confirmed on survival analysis of RFS and OS, and results were consistent (*Figure 4*). Among patients who recurred, patients with 20% or greater CGP trended with a worse post-recurrence survival (PRS) than those with less than 20% CGP (3-year PRS, 45% versus 70%, respectively; $P=0.0053$). RFS in patients with recurrence was also compared and patients with 20% or greater CGP exhibit a faster recurrence pattern than those with less than 20% CGP (mean RFS, 18.77 versus 14.47 months, respectively; $P=0.0395$) (*Figure 4*).

Univariable and multivariable Cox regression model were performed. Variables identified as risk factors in univariate analysis were enrolled in multivariate Cox analysis. Solid and micropapillary patterns were recognized as high-grade patterns together with CGP, therefore we added solid and micropapillary patterns into the analysis. Given the significant correlation between CGP and pTNM staging, they were separately included in two multivariate analyses while the other variables were fixed. CGP (≥20% vs. <20%, $P<0.001$), smoking history (positive vs. negative, $P<0.001$), pT stage (T2–4 vs. T1, $P=0.011$), pN stage (N1–3 vs. N0,

Table 1 Associations of complex glandular pattern (CGP) with clinical characteristics

Variables	0–19%, n=387 (%)	20–100%, n=563 (%)	P
Age, mean (range)	60.6 (26.5, 83)	60.3 (23.4, 84)	0.578
Sex			0.004
Male	150 (38.8)	271 (48.1)	
Female	237 (61.2)	292 (51.9)	
Smoking history			<0.001
Never	325 (84.0)	408 (72.5)	
Ever	62 (16.0)	155 (27.5)	
CT manifestation			<0.001
Solid nodule	153 (39.5)	448 (79.6)	
Part/non-solid nodule	234 (60.5)	115 (20.4)	
Surgery			<0.001
Lobectomy or more	355 (91.7)	550 (97.7)	
Sublobar resection	32 (8.3)	13 (2.3)	
p-TNM stage			<0.001
I	336 (86.8)	299 (53.1)	
II	18 (4.7)	55 (9.8)	
III	33 (8.5)	209 (37.1)	
T stage			<0.001
T1	323 (83.5)	343 (61.0)	
T2	54 (14.0)	171 (30.4)	
T3	9 (2.3)	42 (7.5)	
T4	1 (0.3)	7 (1.2)	
N status			<0.001
N0	349 (90.2)	326 (57.9)	
N1	7 (2.0)	34 (6.0)	
N2	31 (8.0)	195 (34.6)	
N3	0 (0)	8 (1.4)	
Visceral pleural invasion			<0.001
Absent	324 (83.7)	428 (76.0)	
Present	63 (16.3)	135 (23.0)	
Lymphatic invasion			<0.001
Absent	370 (95.6)	443 (78.7)	
Present	17 (4.4)	120 (21.3)	
Adjuvant therapies			<0.001
Absent	312 (80.6)	266 (47.2)	
Present	75 (19.4)	297 (52.8)	

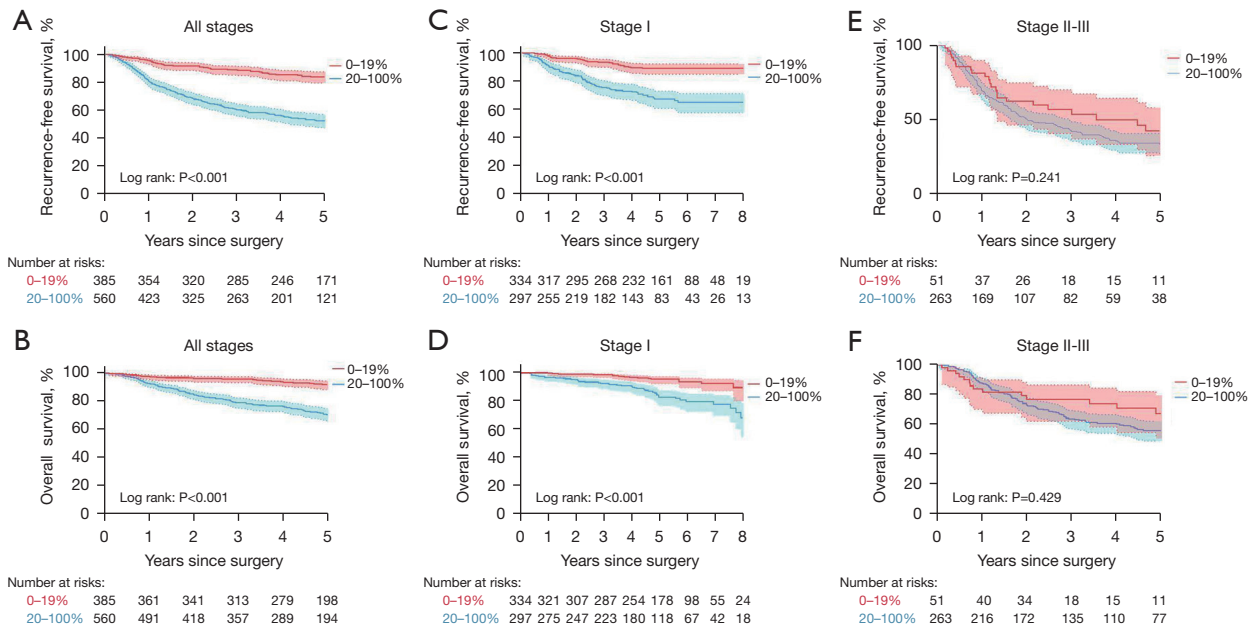


Figure 3 Prognostic significance of different proportion of CGP, (A,B) RFS and OS curve of patients with 0–19% and 20–100% CGP; (C,D) RFS and OS curve of stage I patients with 0–19% and 20–100% CGP; (E,F) RFS and OS curve of stage II-III patients with 0–19% and 20–100% CGP; Error bars were displayed at 95% confidence limits; RFS, recurrence-free survival; OS, overall survival; CGP, complex glandular pattern.

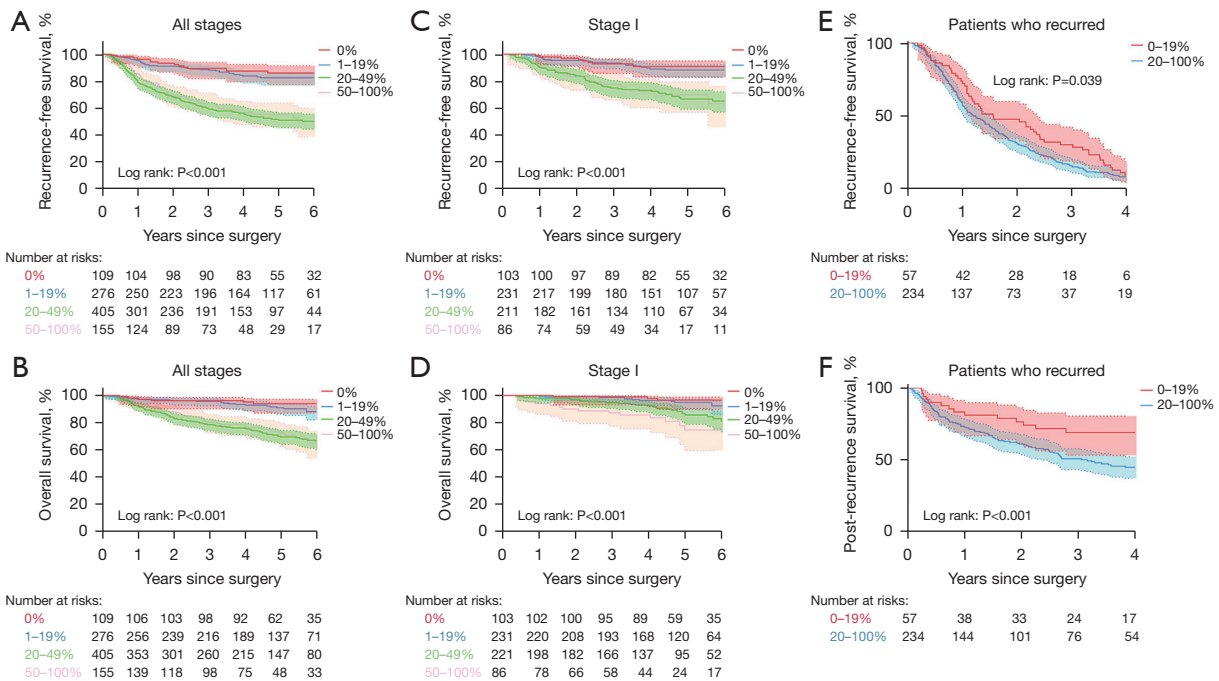


Figure 4 Prognostic significance of different proportion of CGP in stage I patients: (A,B) RFS and OS curve of patients with 0%, 1–19%, 20–49% and 50–100% CGP; (C,D) RFS and OS curve of stage I patients with 0%, 1–19%, 20–49% and 50–100% CGP; (E,F) RFS and PRS in patients who recurred with 0–19% and 20–100% CGP; Error bars were displayed at 95% confidence limits; RFS, recurrence-free survival; OS, overall survival; PRS, post-recurrence survival; CGP, complex glandular pattern.

Table 2 Univariable and multivariable cox analysis for RFS using cox regression hazards model

Cox (RFS)	Univariable		Multivariable1		Multivariable2	
	HR (95% CI)	P	HR (95% CI)	P	HR (95% CI)	P
Gender (male vs. female)	0.724 (0.576, 0.909)	0.005	0.962 (0.720, 1.284)	0.791	0.914 (0.686, 1.219)	0.541
Age	0.996 (0.985, 1.008)	0.594				
Smoking history (ever vs. never)	1.838 (1.433, 2.357)	0.000	1.585 (1.236, 2.032)	0.000	1.514 (1.179, 1.944)	0.001
pT stage (T2-4 vs. T1)	2.967 (2.360, 3.730)	0.000	1.111 (0.813, 1.517)	0.508	1.419 (1.083, 1.859)	0.011
pN stage (N1-3 vs. N0)	4.361 (3.461, 5.496)	0.000	1.024 (0.621, 1.691)	0.925	2.457 (1.827, 3.296)	0.000
pTNM stage (stage II-IV vs. stage I)	4.793 (3.789, 6.064)	0.000	3.379 (2.577, 4.430)	0.000		
Visceral pleural invasion (presence vs. absence)	1.844 (1.433, 2.372)	0.000	1.308 (1.013, 1.690)	0.040	1.170 (0.884, 1.548)	0.272
Lymphovascular invasion (presence vs. absence)	3.227 (2.475, 4.207)	0.000	1.467 (1.103, 1.950)	0.008	1.415 (1.062, 1.884)	0.018
Gene mutational status (<i>EGFR</i> vs. wild type)	1.248 (0.913, 1.705)	0.164				
Gene mutational status (<i>KRAS</i> vs. wild type)	1.542 (0.908, 2.621)	0.109				
Gene mutational status (<i>ALK</i> vs. wild type)	1.704 (0.886, 3.278)	0.110				
Gene mutational status (<i>HER2</i> vs. wild type)	1.689 (0.526, 5.421)	0.378				
Solid pattern (presence vs. absence)	2.292 (1.822, 2.884)	0.000	1.374 (1.079, 1.750)	0.010	1.197 (0.938, 1.529)	0.149
Micropapillary pattern (presence vs. absence)	2.001 (1.563, 2.561)	0.000	1.364 (1.056, 1.762)	0.018	1.184 (0.906, 1.546)	0.091
Complex glandular pattern (20–100% vs. 0–19%)	3.910 (2.905, 5.261)	0.000			2.197 (1.616, 2.988)	0.000

RFS, recurrence-free survival; HR, hazard ratio; T, tumor; N, node; TNM, tumor node metastasis; *EGFR*, epidermal growth factor receptor; *KRAS*, Kirsten rat sarcoma; *ALK*, anaplastic lymphoma kinase; *HER2*, human epidermal growth factor receptor 2.

$P < 0.001$) and LVI ($P = 0.018$) were significantly associated with RFS after adjustment for the other risk factors (Table 2). CGP ($\geq 20\%$ vs. $< 20\%$, $P < 0.001$), pN stage (N1-3 vs. N0, $P < 0.001$), *EGFR* mutation (Wild Type vs. Mutation, $P = 0.020$), *HER2* kinase domain mutations (Mutation vs. Wild Type, $P < 0.001$) and solid pattern (presence vs. absence, $P = 0.020$) were determined as independent predictors for OS (Table 3).

Mutational profile and its correlation with CGP

All patients in this cohort ($n = 950$) were sequenced for hot-spot regions of seven common driver mutations and fusions (*EGFR*, *KRAS*, *ALK*, *HER2*, *BRAF*, *ROS1*, and *RET*). There were 210 patients with no detected mutation. The most frequent driver mutation in this cohort was *EGFR* and was detected in 624 (65.7%) patients. Other mutations were comprehensively analyzed, there were 55 *KRAS* mutations, 26 *ALK* fusions, 9 *HER2* kinase domain mutations, 14 *RET* fusions, 9 *BRAF* mutations and 3 *ROS1* fusions, respectively. Common driver mutations status and its distribution in

different CGP was analyzed and demonstrated in Figure 5. Due to their small numbers, *BRAF* mutation, *ROS1* and *RET* fusion were grouped as “Others”. *EGFR* mutation were more frequently observed in patients with $< 20\%$ CGP (73.6% vs. 60.2%, $P < 0.001$). CGP ($\geq 20\%$) was significantly associated with *KRAS* mutation and *ALK* rearrangement ($P = 0.001$ and $P = 0.006$, respectively) (Table 4). Due to the correlations, OS and RFS regarding mutational status of *EGFR*, *ALK* fusion and *KRAS* irrespective of CGP percent were also analyzed and we found that there was no significant difference in prognosis of *EGFR*+, *KRAS*+ and *ALK* fusion+ patients. Yet, we found that *EGFR* positive patients has a better OS than *EGFR* negative patients (Figure 6; $P < 0.001$).

In this cohort, *EGFR* mutation is found to be correlated with $< 20\%$ CGP. Therefore, we analyzed the prognostic significance of CGP in a subgroup of *EGFR*-positive patients (Figure 7). Results were consistent with the whole cohort.

Discussion

Ever since Moreira *et al.* reported cribriform pattern and

Table 3 Univariable and multivariable cox analysis for OS using cox regression hazards model

Cox (OS)	Univariable		Multivariable1		Multivariable2	
	HR (95% CI)	P	HR (95% CI)	P	HR (95% CI)	P
Gender (male vs. female)	0.793 (0.594, 1.058)	0.115				
Age	1.012 (0.997, 1.027)	0.132				
Smoking history (ever vs. never)	1.561 (1.142, 2.133)	0.005	1.286 (0.931, 1.778)	0.127	1.265 (0.915, 1.747)	0.155
pT stage (T2-4 vs. T1)	3.044 (2.280, 4.063)	0.000	1.121 (0.788, 1.595)	0.525	1.311 (0.940, 1.829)	0.110
pN stage (N1-3 vs. N0)	5.295 (3.932, 7.130)	0.000	1.573 (0.827, 2.990)	0.167	3.921 (2.846, 5.401)	0.000
pTNM stage (stage II-IV vs. stage I)	5.583 (4.100, 7.602)	0.000	4.462 (3.174, 6.272)	0.000		
Visceral pleural invasion (presence vs. absence)	1.452 (1.051, 2.004)	0.024	1.062 (0.737, 1.531)	0.745	1.024 (0.714, 1.469)	0.899
Lymphovascular invasion (presence vs. absence)	3.106 (2.252, 4.285)	0.000	1.506 (1.069, 2.123)	0.019	1.301 (0.917, 1.845)	0.140
Gene mutational status (<i>EGFR</i> vs. wild type)	0.651 (0.454, 0.933)	0.019	0.682 (0.501, 0.929)	0.015	0.672 (0.484, 0.934)	0.018
Gene mutational status (<i>KRAS</i> vs. wild type)	1.032 (0.533, 0.926)	0.922	0.851 (0.458, 1.581)	0.658	0.819 (0.441, 1.521)	0.528
Gene mutational status (<i>ALK</i> vs. wild type)	1.184 (0.556, 2.524)	0.661	0.746 (0.353, 1.576)	0.340	0.696 (0.325, 1.487)	0.349
Gene mutational status (<i>HER2</i> vs. wild type)	3.893 (1.654, 9.161)	0.002	6.066 (2.614, 14.078)	0.000	5.926 (2.553, 13.758)	0.000
Solid pattern (presence vs. absence)	2.775 (2.078, 3.706)	0.034	1.582 (1.157, 2.165)	0.004	1.448 (1.061, 1.976)	0.020
Micropapillary pattern (presence vs. absence)	1.890 (1.383, 2.583)	0.000	1.232 (0.889, 1.707)	0.209	1.066 (0.758, 1.498)	0.714
Complex glandular pattern (20–100% vs. 0–19%)	3.910 (2.905, 5.261)	0.000			2.123 (1.400, 3.220)	0.000

OS, overall survival; HR, hazard ratio; T, tumor; N, node; TNM, tumor node metastasis; *EGFR*, epidermal growth factor receptor; *KRAS*, Kirsten rat sarcoma; *ALK*, anaplastic lymphoma kinase; *HER2*, human epidermal growth factor receptor 2.

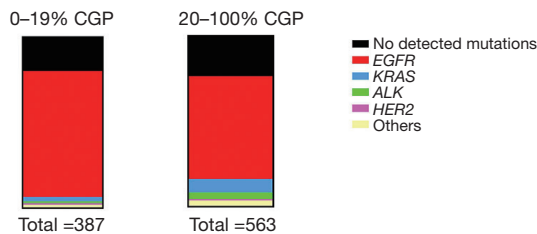


Figure 5 Mutational profile of patients with 0–19% and 20–100% CGP; CGP, complex glandular pattern; *EGFR*, epidermal growth factor receptor; *KRAS*, Kirsten rat sarcoma; *ALK*, anaplastic lymphoma kinase; *HER2*, human epidermal growth factor receptor 2.

fused gland as a novel pathological pattern (12), there has been researches on CGP. Earlier studies have given different results regarding the association between CGP and gene alterations (6,8,9,12,15), mainly due to the small population and unavailable mutation status. Our study, which was based on Asian population, found that patients with 20% or less CGP component harbor *EGFR* mutation

Table 4 Associations of complex glandular pattern (CGP) with gene mutation status

Variables	0–19%, n=387 (%)	20–100%, n=563 (%)	P
Gene mutation status			
Wild type	76 (19.6)	132 (23.4)	0.164
<i>EGFR</i> -positive	285 (73.6)	339 (60.2)	<0.001
<i>KRAS</i> -positive	10 (2.6)	45 (8.0)	0.001
<i>ALK</i> -positive	4 (1.0)	22 (4.0)	0.013
<i>HER2</i> -positive	4 (1.0)	5 (0.9)	0.820
Others	8 (2.1)	20 (3.6)	0.184

EGFR, epidermal growth factor receptor; *KRAS*, Kirsten rat sarcoma; *ALK*, anaplastic lymphoma kinase; *HER2*, human epidermal growth factor receptor 2.

at a considerable rate than their counterparts. We also found that *KRAS* mutation and *ALK* rearrangements were positively associated with CGP. This gives implications for clinical therapeutic strategies. Due to the different

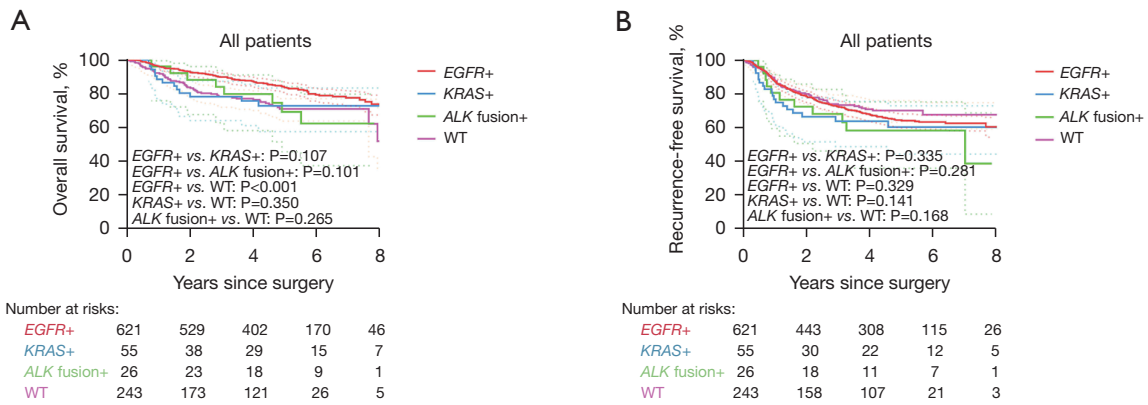


Figure 6 Prognosis of patients with *EGFR* mutations, *KRAS* mutations, *ALK*-fusion and none above mutations (WT). (A,B) RFS and OS curve of patients with *EGFR* mutations, *KRAS* mutations, *ALK*-fusion and none above mutations (WT). RFS, recurrence-free survival; OS, overall survival; *EGFR*, epidermal growth factor receptor; *KRAS*, Kirsten rat sarcoma; *ALK*, anaplastic lymphoma kinase; WT, wild type.

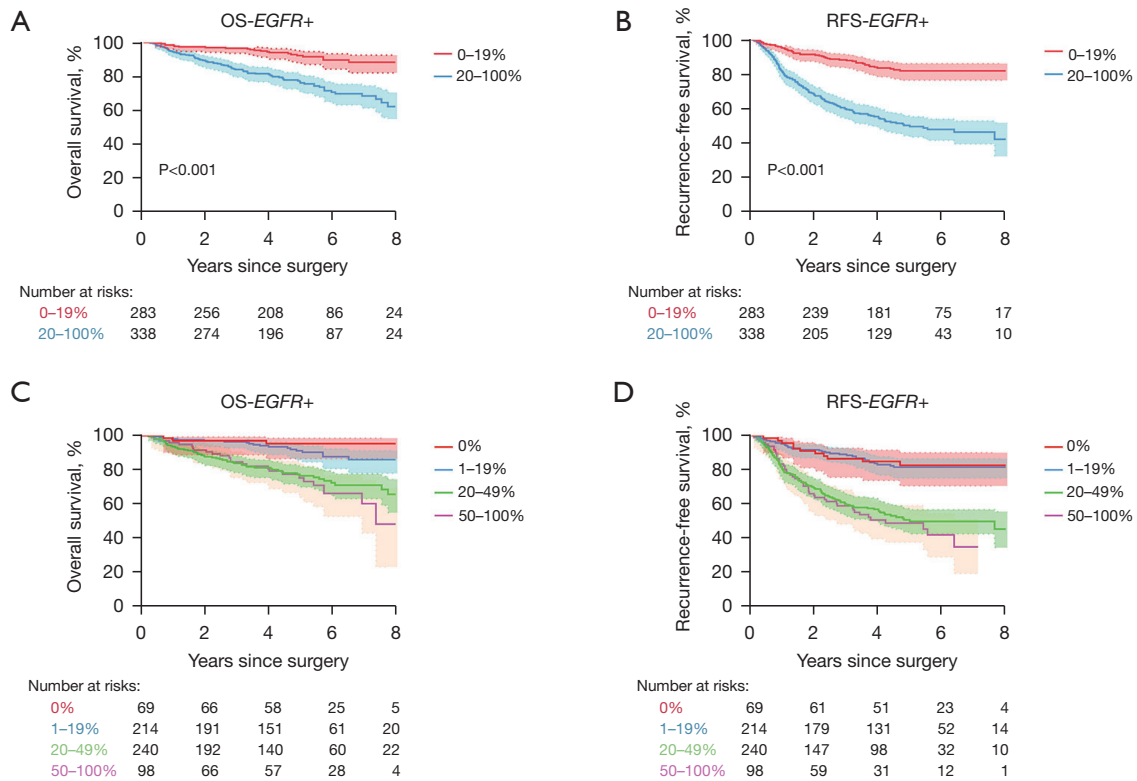


Figure 7 Prognostic significance of different proportion of CGP in *EGFR*+ patients. (A,B) RFS and OS curve of *EGFR*+ patients with 0-19%, and 20-100% CGP; (C,D) RFS and OS curve of *EGFR*+ patients with 0%, 1-19%, 20-49% and 50-100% CGP. Error bars were displayed at 95% confidence limits. RFS, recurrence-free survival; OS, overall survival; *EGFR*, epidermal growth factor receptor; CGP, complex glandular pattern.

correlation between *EGFR* mutation, *KRAS* mutation and *ALK* rearrangements, we performed survival analysis on different mutational status of patients in our cohort irrespective of CGP component and we found that there was no significant difference in prognosis of *EGFR*+, *KRAS*+ and *ALK* fusion+ patients even though they had different relevance with CGP. Meanwhile, we found that *EGFR* positive patients has a better OS than *EGFR* negative patients. We perceive this as a result of development of *EGFR*-TKIs in the treatment of lung adenocarcinoma, this was also consistent with our previous research (16) in which we found that *EGFR*-positive patients have a better OS when analyzed in an unmodified cohort. It seems that the association between specific gene variations and complex glandular growth pattern is still controversial, and further studies should be performed.

Our results were consistent with previous studies with regard to the prognostic value of CGP in lung adenocarcinoma. Moreira *et al.* found that patients with CGP tumors had lower 5-year recurrence-free probability than intermediate and low-grade patients in an American population (12). Warth *et al.* reported complex glandular predominant tumor was associated with the worst RFS of all patterns based on a German cohort (7). In our cohort of Asian patients, CGP ($\geq 20\%$) was significantly associated with worse RFS (mean RFS: 36.4 *vs.* 52.8 months, $P < 0.001$) and OS (mean OS: 47.6 *vs.* 57.4 months, $P < 0.001$).

The 2015 IASLC/American Thoracic Society (ATS)/European Respiratory Society (ERS) classification system recommends the recording of histologic patterns semi-quantitatively in 5% increments (4). Previous studies utilize different cut-off value of cribriform component to distinguish its aggressive behavior. Kadota *et al.* divided the patients into three groups: $< 10\%$, 10–39%, and $\geq 40\%$. They found that RFS difference was not significant between 10–39% and $\geq 40\%$, and was significant between 10–39% and $< 10\%$ (17). Thus, 10% was used as cut-off value. Other studies regarded 5% as cribriform present and found that the difference in RFS and OS was significant (9,18). Studies relating CGP seldom utilize cut-off value, they used most predominant portion instead (5,12,15). The newly proposed grading system (10) had included cribriform and fused gland into CGPs as high-grade and proposed that any tumor with 20% or more of high-grade patterns be classified as poorly differentiated. Unlike solid or micro-papillary subtype, lack of appreciation of CGP may pose uncertainty on establishment of a cutoff value for high-grade pattern. Also, the new system regard high grade

pattern as a whole and there has not been an individual investigation on CGPs. In this study, we found that the group without CGP and the group with 5–15% CGP is comparable in RFS and OS. There was also no significant difference in RFS and OS between 20–45% and 50–100%. Thus, 20% as the cut-off value seems to be solid for distinguishing the aggressive behavior of CGP.

The complex glandular type has been demonstrated to be highly aggressive. Ding *et al.* reported that the cribriform component was an independent risk factor for the presence of spread through air spaces (STAS) (18). Furthermore, mucin production is often presence in cribriform pattern, providing evidence for its aggressive behavior (8). However, little progress has been made to described the molecular alterations that occur in the complex glandular morphological pattern.

There are several limitations of this study. First, the follow-up duration for estimating RFS and OS may not be long enough. Second, like other single institution-based, retrospective, observational cohort studies, there was potential for referral and selection bias. Third, our study categorized the component of CGP into four groups, and tested the cut-off value of 0%, 20% and 50%, more detailed analyzation of CGP may be needed to explore a better cut-off value.

In conclusion, our study provided mutational profile of patients with different CGP, validated the poor prognosis associated with CGP and supplied further evidence of proper cut-off value, giving insights on the clinical management of patients with CGP.

Acknowledgments

Funding: This work was supported by the National Natural Science Foundation of China (Nos. 81930073, 81972171, 81772466), Shanghai Municipal Science and Technology Major Project (Nos. 2017SHZDZX01, VBH1323001/026), Shanghai Municipal Key Clinical Specialty Project (No. SHSLCZDZK02104), Shanghai Technology Innovation Action Project (No. 20JC1417200), Pilot Project of Fudan University (No. IDF159045) and Shanghai Rising-Star Program (No. 21QC1400600).

Footnote

Reporting Checklist: The authors have completed the REMARK reporting checklist. Available at <https://tclr.amegroups.com/article/view/10.21037/tclr-22-127/rc>

Data Sharing Statement: Available at <https://tcr.amegroups.com/article/view/10.21037/tcr-22-127/dss>

Conflicts of Interest: All authors have completed the ICMJE uniform disclosure form (available at <https://tcr.amegroups.com/article/view/10.21037/tcr-22-127/coif>). The authors have no conflicts of interest to declare.

Ethical Statement: The authors are accountable for all aspects of the work in ensuring that questions related to the accuracy or integrity of any part of the work are appropriately investigated and resolved. The study was conducted in accordance with the Declaration of Helsinki (as revised in 2013). This study was approved by the institutional review board (Fudan University Shanghai Cancer Center IRB 2008223-9, date: 2020/07/14). Informed consents were waived because it was a retrospective study.

Open Access Statement: This is an Open Access article distributed in accordance with the Creative Commons Attribution-NonCommercial-NoDerivs 4.0 International License (CC BY-NC-ND 4.0), which permits the non-commercial replication and distribution of the article with the strict proviso that no changes or edits are made and the original work is properly cited (including links to both the formal publication through the relevant DOI and the license). See: <https://creativecommons.org/licenses/by-nc-nd/4.0/>.

References

1. Siegel RL, Miller KD, Jemal A. Cancer statistics, 2019. *CA Cancer J Clin* 2019;69:7-34.
2. Goldstraw P, Chansky K, Crowley J, et al. The IASLC Lung Cancer Staging Project: Proposals for Revision of the TNM Stage Groupings in the Forthcoming (Eighth) Edition of the TNM Classification for Lung Cancer. *J Thorac Oncol* 2016;11:39-51.
3. Marx A, Chan JK, Coindre JM, et al. The 2015 World Health Organization Classification of Tumors of the Thymus: Continuity and Changes. *J Thorac Oncol* 2015;10:1383-95.
4. Travis WD, Brambilla E, Nicholson AG, et al. The 2015 World Health Organization Classification of Lung Tumors: Impact of Genetic, Clinical and Radiologic Advances Since the 2004 Classification. *J Thorac Oncol* 2015;10:1243-60.
5. Kadota K, Kushida Y, Kagawa S, et al. Cribriform Subtype is an Independent Predictor of Recurrence and Survival After Adjustment for the Eighth Edition of TNM Staging System in Patients With Resected Lung Adenocarcinoma. *J Thorac Oncol* 2019;14:245-54.
6. Qu Y, Lin H, Zhang C, et al. Cribriform pattern in lung invasive adenocarcinoma correlates with poor prognosis in a Chinese cohort. *Pathol Res Pract* 2019;215:347-53.
7. Warth A, Muley T, Kossakowski C, et al. Prognostic impact and clinicopathological correlations of the cribriform pattern in pulmonary adenocarcinoma. *J Thorac Oncol* 2015;10:638-44.
8. Yang F, Dong Z, Shen Y, et al. Cribriform growth pattern in lung adenocarcinoma: More aggressive and poorer prognosis than acinar growth pattern. *Lung Cancer* 2020;147:187-92.
9. Zhang R, Hu G, Qiu J, et al. Clinical significance of the cribriform pattern in invasive adenocarcinoma of the lung. *J Clin Pathol* 2019;72:682-8.
10. Moreira AL, Ocampo PSS, Xia Y, et al. A Grading System for Invasive Pulmonary Adenocarcinoma: A Proposal From the International Association for the Study of Lung Cancer Pathology Committee. *J Thorac Oncol* 2020;15:1599-610.
11. Rokutan-Kurata M, Yoshizawa A, Ueno K, et al. Validation Study of the International Association for the Study of Lung Cancer Histologic Grading System of Invasive Lung Adenocarcinoma. *J Thorac Oncol* 2021;16:1753-8.
12. Moreira AL, Joubert P, Downey RJ, et al. Cribriform and fused glands are patterns of high-grade pulmonary adenocarcinoma. *Hum Pathol* 2014;45:213-20.
13. Deng C, Zheng Q, Zhang Y, et al. Validation of the Novel International Association for the Study of Lung Cancer Grading System for Invasive Pulmonary Adenocarcinoma and Association With Common Driver Mutations. *J Thorac Oncol* 2021;16:1684-93.
14. Pan Y, Zhang Y, Ye T, et al. Detection of Novel NRG1, EGFR, and MET Fusions in Lung Adenocarcinomas in the Chinese Population. *J Thorac Oncol* 2019;14:2003-8.
15. Kuang M, Shen X, Yuan C, et al. Clinical Significance of Complex Glandular Patterns in Lung Adenocarcinoma: Clinicopathologic and Molecular Study in a Large Series of Cases. *Am J Clin Pathol* 2018;150:65-73.
16. Deng C, Zhang Y, Ma Z, et al. Prognostic value of epidermal growth factor receptor gene mutation in resected lung adenocarcinoma. *J Thorac Cardiovasc Surg* 2021;162:664-674.e7.
17. Kadota K, Yeh YC, Sima CS, et al. The cribriform pattern identifies a subset of acinar predominant tumors with poor prognosis in patients with stage I lung adenocarcinoma: a conceptual proposal to classify cribriform predominant

- tumors as a distinct histologic subtype. *Mod Pathol* 2014;27:690-700.
18. Ding Q, Chen D, Wang X, et al. Characterization of lung

adenocarcinoma with a cribriform component reveals its association with spread through air spaces and poor outcomes. *Lung Cancer* 2019;134:238-44.

Cite this article as: Bai J, Deng C, Zheng Q, Li D, Fu F, Li Y, Zhang Y, Chen H. Comprehensive analysis of mutational profile and prognostic significance of complex glandular pattern in lung adenocarcinoma. *Transl Lung Cancer Res* 2022;11(7):1337-1347. doi: 10.21037/tlcr-22-127

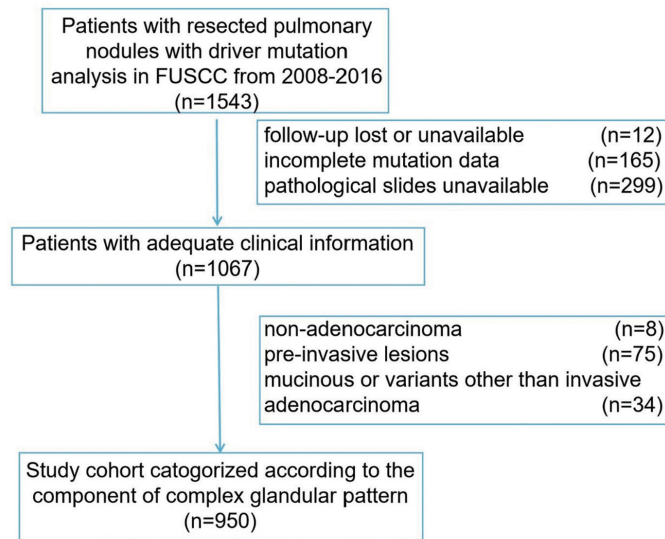


Figure S1 Diagram of patient recruitment. FUSCC, Fudan University Shanghai Cancer Center.

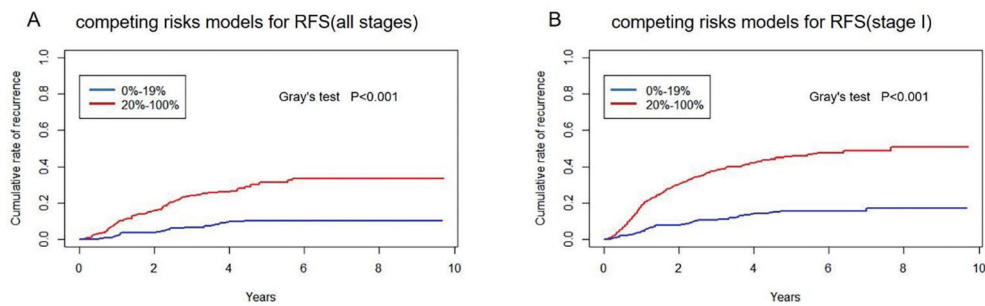


Figure S2 Cumulative incidence rate of recurrence according to CGP component. (A) Cumulative incidence rate of recurrence for all patients according to CGP component (0–19% and 20–100%); (B) cumulative incidence rate of recurrence for stage I patients according to CGP component (0–19% and 20–100%); CGP, complex glandular pattern; RFS, recurrence-free survival.